ARL-MR-1043 ● SEP 2021

DEVCOM ARMY RESEARCH LABORATORY

Approaches to Mechanical Reduction of Dispersion in Blast Measurements Using Kolsky Bars

by David Fox

Approved for public release: distribution unlimited.

NOTICES

Disclaimers

The findings in this report are not to be construed as an official Department of the Army position unless so designated by other authorized documents.

Citation of manufacturer's or trade names does not constitute an official endorsement or approval of the use thereof.

Destroy this report when it is no longer needed. Do not return it to the originator.

ARL-MR-1043 ● SEP 2021



Approaches to Mechanical Reduction of Dispersion in Blast Measurements Using Kolsky Bars

David Fox
Weapons Material and Research Directorate,
DEVCOM Army Research Laboratory

Approved for public release: distribution unlimited.

REPORT DOCUMENTATION PAG	*Form Approved OMB No. 0704-0188*

Public reporting burden for this collection of information is estimated to average 1 hour per response, including the time for reviewing instructions, searching existing data sources, gathering and maintaining the data needed, and completing and reviewing the collection information. Send comments regarding this burden estimate or any other aspect of this collection of information, including suggestions for reducing the burden, to Department of Defense, Washington Headquarters Services, Directorate for Information Operations and Reports (0704-0188), 1215 Jefferson Davis Highway, Suite 1204, Arlington, VA 22202-4302. Respondents should be aware that notwithstanding any other provision of law, no person shall be subject to any penalty for failing to comply with a collection of information if it does not display a currently valid OMB control number.
PLEASE DO NOT RETURN YOUR FORM TO THE ABOVE ADDRESS.

1. REPORT DATE *(DD-MM-YYYY)*	2. REPORT TYPE	3. DATES COVERED (From - To)
September 2021	Technical Report	1 October 2020–9 September 2021

4. TITLE AND SUBTITLE	5a. CONTRACT NUMBER
Approaches to Mechanical Reduction of Dispersion in Blast Measurements Using Kolsky Bars	5b. GRANT NUMBER
	5c. PROGRAM ELEMENT NUMBER

6. AUTHOR(S)	5d. PROJECT NUMBER
David Fox	5e. TASK NUMBER
	5f. WORK UNIT NUMBER

7. PERFORMING ORGANIZATION NAME(S) AND ADDRESS(ES)	8. PERFORMING ORGANIZATION REPORT NUMBER
DEVCOM Army Research Laboratory ATTN: FCDD-RLW-TG Aberdeen Proving Ground MD 21005	ARL-MR-1043

9. SPONSORING/MONITORING AGENCY NAME(S) AND ADDRESS(ES)	10. SPONSOR/MONITOR'S ACRONYM(S)
	11. SPONSOR/MONITOR'S REPORT NUMBER(S)

12. DISTRIBUTION/AVAILABILITY STATEMENT

Approved for public release: distribution unlimited.

13. SUPPLEMENTARY NOTES

14. ABSTRACT

Cylindrical Kolsky bars offer an attractive means for measuring time-varying blast pressure fields, but their accuracy is often compromised due to dispersion effects from high-frequency stresses resulting from Poisson's effect, which propagates in the bars' radial direction. Radial stresses distort the axial strain signal due to the inertial effects they induce in the bar's longitudinal direction. Using appropriate bar geometry can reduce some of the inaccuracies. In addition, analytical and numerical methods have been devised that can, in some situations, improve blast measurement accuracy. Here, we demonstrate, using computational methods, the efficacy of two more direct approaches that involve applying mechanical means to suppress blast pressure signal inaccuracy. The first approach uses beryllium, which has an extremely low Poisson ratio of 0.03, as the bar material to reduce signal distortion due to dispersion. The second method uses mechanical constraint in the radial direction to suppress the noise in the pressure signal. Initial computational evaluations of this technique used an annular sheath in intimate contact with the outer radius of the bottom section of the bar. Using a Teflon sheath reduced the overprediction of peak blast pressure from a level of 12%, the baseline level for an unconfined bar, to 3%.

15. SUBJECT TERMS

blast measurement, Kolsky bar, signal dispersion, pressure measurement, explosive blast, pressure waves

16. SECURITY CLASSIFICATION OF:			17. LIMITATION OF ABSTRACT	18. NUMBER OF PAGES	19a. NAME OF RESPONSIBLE PERSON
a. REPORT	b. ABSTRACT	c. THIS PAGE			David Fox
Unclassified	Unclassified	Unclassified	UU	27	19b. TELEPHONE NUMBER (Include area code) (410) 278-6033

Standard Form 298 (Rev. 8/98)
Prescribed by ANSI Std. Z39.18

Contents

List of Figures iv

1. Introduction 1

2. Computational Method and Constitutive Models 6

2.1 Computational Method 6

2.2 Constitutive Models 8

3. Results and Discussion 9

3.1 Radial Direction Displacement Constraints 9

3.2 Beryllium Kolsky Bars 10

3.3 Windowed Radial Constraint 12

3.4 Kolsky Bar Sheath Radial Constraints 15

4. Summary and Conclusions 17

5. References 19

Distribution List 21

List of Figures

Fig. 1 Schematic of a typical Kolsky bar setup (not to scale) for measurement of a spatially and temporally varying pressure field caused by an explosive confined in soil or metal particles..... 2

Fig. 2 Experimental pressure pulse for an explosive charge buried in dry sand measured by means of a Kolsky bar[4] 3

Fig. 3 Effects of dispersion on Kolsky bar strain gauge measurement of a typical pressure signal waveform. The Kolsky bar signals were shifted in time to allow a closer comparison between them and the input signal. 4

Fig. 4 Kolsky bar arrangement used for computations 7

Fig. 5 Input pressure pulses that were applied uniformly to the bottom flat surfaces of the Kolsky bars. The amplitudes and durations of the pulses were varied to match the purpose of the analysis in which they were used. 8

Fig. 6 Influence of constraint in the radial direction, at the outer radius of the C350 maraging steel Kolsky bar, on the accuracy of reproduction of the exponential sine input pressure signal with a peak amplitude of 345 MPa 10

Fig. 7 Beryllium Kolsky bars improve signal measurement. The Kolsky bar signals were shifted in time to allow a closer comparison between them and the 170-MPa peak pressure input signal. 11

Fig. 8 Geometric configuration of a Kolsky bar that is set up to mechanically suppress blast pressure measurement degradation due to dispersion effects 12

Fig. 9 Comparison of measured peak pressure calculated by converting the peak longitudinal strain to stress using the constrained modulus M for C350 steel (270 MPa) and the measured peak pressure using an adjusted constrained modulus M' (290 MPa) 13

Fig. 10 Comparison of input pressure signal, windowed constraint C350 maraging steel Kolsky bar, and traditional unconstrained Kolsky bar responses to 345-GPa peak exponential sine signal pressure input 14

Fig. 11 Windowed constraint C350 maraging steel Kolsky bar and traditional unconstrained Kolsky bar responses to 345-GPa peak square wave pressure input 15

Fig. 12 Comparison of computational pressure–time histories measured using unconstrained bars with those measured with bars sheathed at their bottoms with 3.075-mm-thick annuli of Teflon, C350 maraging steel, or heavy tungsten alloy 16

Fig. 13 The effect of increasing the thickness of the constraining Teflon sleeve from 3.075 to 6 mm 17

1. Introduction

A detailed understanding of the nature of the stress and momentum created by blasts significantly improves the potential for the effective design of active and passive protection systems against such environments. Such an understanding also facilitates the capability for lower-cost design of protective treatments by increasing the accuracy of computational models. As a result, it is useful to devise and perform controlled experiments that involve pressure measurement to better understand the evolution of the types of loading that would be expected to impact relevant objects.

The nature of many blast events, particularly those that involve mixtures of air, detonation, products, and entrained solid particles, such as soil or metal fragments, are often such that standard pressure sensors, force sensors, and accelerometers cannot be used to accomplish accurate measurement of the associated pressure fields. As a result, cylindrical Kolsky bars have been used to measure these types of blast pressure fields. Blast pressure and specific impulse can be measured by exposing the flat end surface of a cylindrical Kolsky bar to the advancing front of a solid–gas mixture generated by the detonation of a high explosive,[1–3] then using strain gauges or other means to determine the axial strains and, assuming linearly elastic behavior of the bar material, using the elastic properties of the bars to convert the strains to stresses.

A typical setup for Kolsky bar pressure measurement is shown in Fig. 1. In a typical experiment, an explosive charge is placed in a confining medium and detonated. This creates an expanding mixture comprising explosive detonation products and confining media with an associated time-varying stress field. An array of Kolsky bars is inserted into a rigid plate and set up in such a way that it will be able to measure, at various locations of interest, the variation of axial strain over time using strain gauges applied to surfaces at the exterior radii of the Kolsky bars. The elastic properties of the bar material are then used to convert the measured axial strain to pressure. An experimentally generated pressure–time history for a gram-scale explosive buried in dry sand is shown in Fig. 2.[4] No dispersion correction was performed on this signal.

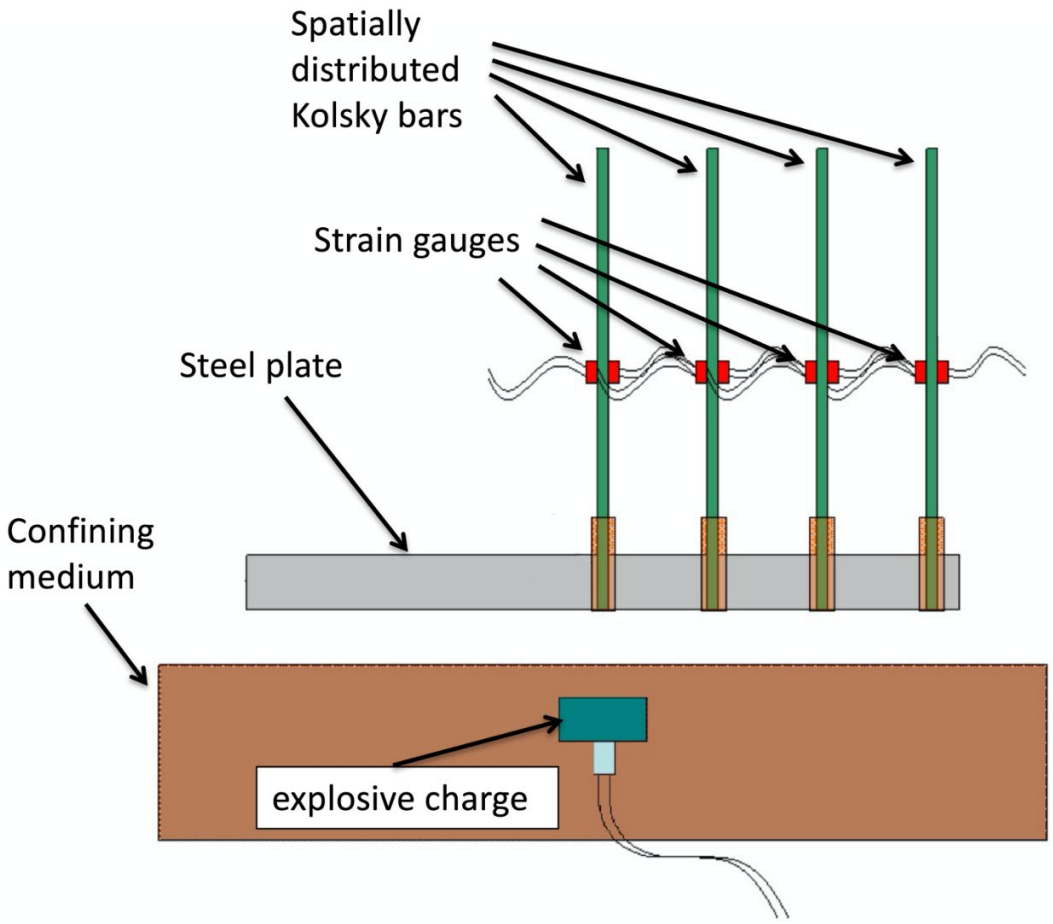


Fig. 1 Schematic of a typical Kolsky bar setup (not to scale) for measurement of a spatially and temporally varying pressure field caused by an explosive confined in soil or metal particles

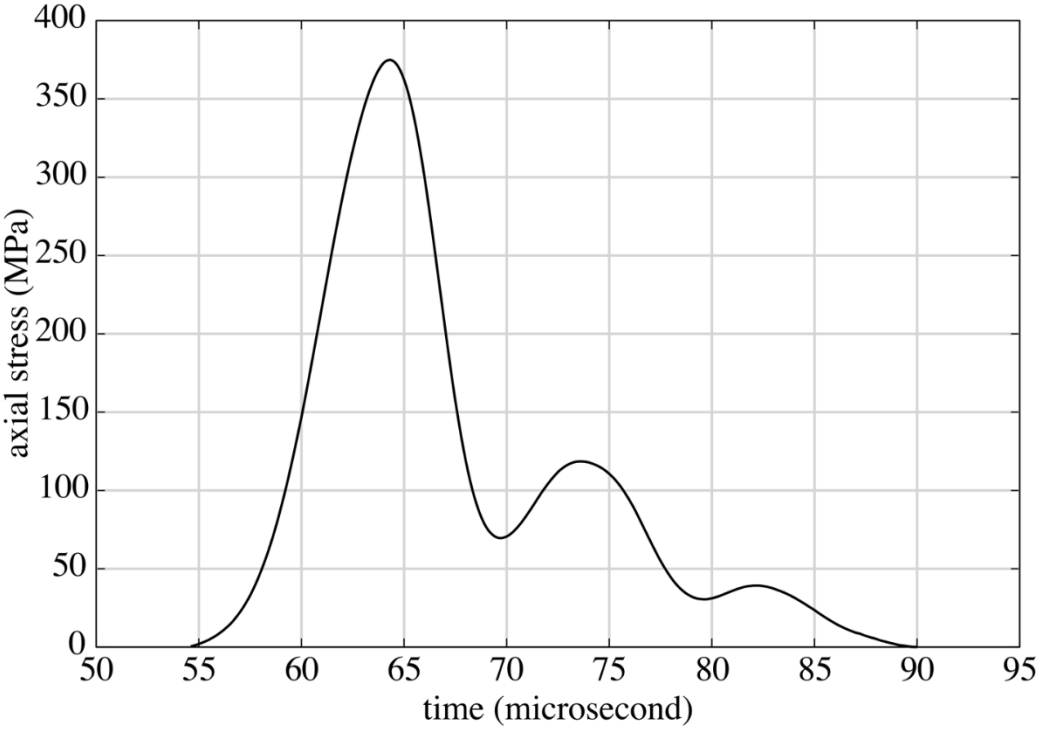


Fig. 2 Experimental pressure pulse for an explosive charge buried in dry sand measured by means of a Kolsky bar[4]

Kolsky bar measurements, particularly at some of the relatively high frequencies associated with blast events, can be significantly affected by pressure signal dispersion in the bars.[5–8] If axial stress signal frequencies are sufficiently high to induce radial stresses via Poisson's effect, then dispersion effects are caused by these radial stresses, which, in turn, induce spurious signals in the longitudinal direction of the bar and distort both the shape and the measured peak values of the pressure–time histories. Although there have been advances in recent decades in instrumentation technology and measurement techniques, the development of more accurate computational models to predict blast events will require an even more precise measurement of the mean values and variability associated with the spatial development of measured experimental blast fields. Improved measurement accuracy would also be expected to improve design methods so that they achieve safer but not overly conservative protective objects. Figure 3, derived using computational techniques, illustrates the effects of Kolsky bar signal dispersion on a known pressure input waveform, as measured at a distance of 15.24 cm (6 inches) from the input signal application surface at the bottom of a Kolsky bar.

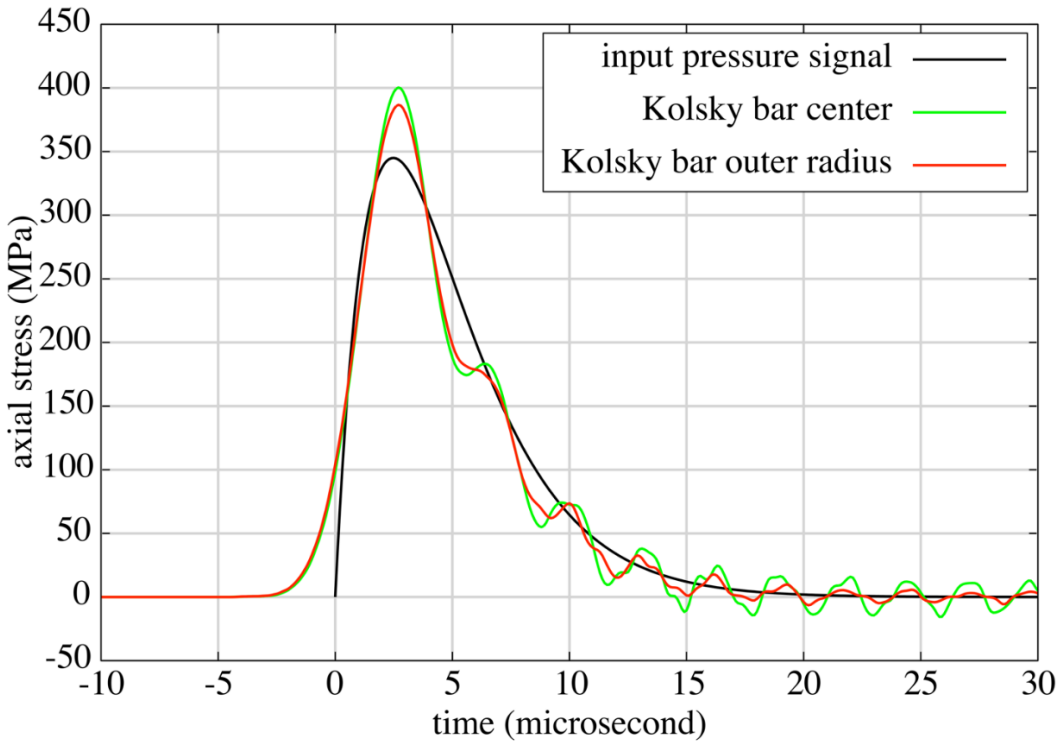


Fig. 3 Effects of dispersion on Kolsky bar strain gauge measurement of a typical pressure signal waveform. The Kolsky bar signals were shifted in time to allow a closer comparison between them and the input signal.

In Fig. 3, the peak input pressure is 345 MPa. The computationally simulated peak pressures, as measured at the center and at the outer radius of the bar and at a distance of 15.24 cm (6 inches) from the signal input surface of the bar, are shown in the green and the red curves, and are somewhat different from each other as well as from those of the input signal. It can be seen that the shapes of the simulated Kolsky bar strain gauge measurements at 15.24 cm also differ from each other as well as from the shape of the input signal. The strain gauge signals were shifted in time to allow a closer comparison between them and the input signal. As a result of signal dispersion and associated oscillations, the apparent peak pressures of the center and outer radius signals, as measured some distance up the bar, are about 12% and 16% higher, respectively, than the peak pressure of the input signal. For this case, use of the measured peak pressure to design a protective object might result in an overly conservative and more expensive product design in terms of both weight and economic cost.

Signals with first-mode dispersion effects, for cases when these effects are dominant, can be treated by using Fourier transform methods to adjust phase velocities in order to improve Kolsky bar pressure measurement accuracy.[9–11] More recently, a hybrid technique that combines Fourier analysis and the finite element

method has been worked out to correct the first four modes of dispersion.[12] Alternatively, it has been shown that, in some cases, dispersion effects can be reduced by appropriate tailoring of the Kolsky bar geometry to the size and frequency content of the blast phenomena to be studied.[13]

In the present work, computational methods are used to demonstrate the possibility of implementing two different approaches to enable mechanical rather than numerical and analytical means to reduce signal dispersion in order to improve the accuracy of Kolsky bar pressure measurement of shock phenomena. Bateman et al.[14] investigated the use of beryllium to raise the upper frequency limit for calibration of accelerometers using Kolsky bars. Beryllium has an extremely low Poisson ratio of 0.03 as well as a very high elastic wave speed by which they hoped to extend the frequency response range of the Kolsky bars they were using for calibration. Their choice of Kolsky bar material suggests the possibility that, due to the extremely low Poisson ratio of beryllium, Kolsky bars constructed from beryllium might have the ability to suppress radial displacements and thereby directly remove dispersion and improve the accuracy of pressure measurement. In the present report, simulations are presented in Section 3.2 that show that, in fact, beryllium Kolsky bars do offer the possibility of dramatic improvement of pressure measurement accuracy.

During the course of analyses that Tyas and Watson[15] performed to investigate various aspects of Kolsky bar behavior, frequency-domain dispersion correction, and sources of numerical errors, they showed the results of a finite element analysis that suppressed radial effects by applying constraints to prevent all nodes in the model from moving in the radial direction. They imposed the constraint boundary conditions to better understand discretization error in their finite element method calculations. The finite element analysis results they presented prompted an idea, although this was not at all discussed in their paper, that there might be an opportunity to reduce or eliminate dispersion by applying radial constraints to Kolsky bars to suppress displacements other than those that occur in the longitudinal direction of the bar. Computations are presented in Section 3.3 that demonstrate the use of a windowed radial constraint method to improve Kolsky bar pressure measurement accuracy. In Section 3.4, simulations are presented of Kolsky bars with 30.48-cm-long sheaths made of Teflon, maraging steel, or heavy tungsten alloy affixed to their outer radii that provide radial direction boundary constraints to the bars.

2. Computational Method and Constitutive Models

2.1 Computational Method

The ALE3D[16] multi-physics package was used to perform Lagrangian simulations of the response of Kolsky bars to time-varying pressure signals applied uniformly to the bottom surface of the bars. A 3-D finite element model with 1/4 symmetry about the longitudinal axis of the bar was used to perform this work. The simulated bars were 121.92 cm (48 inches) long and had a diameter of 0.635 cm (1/4 inch), the typical dimensions of Kolsky bars used for this type of applications. The finite element mesh comprised 10,424,160 hexahedral elements with a nominal element side length of 0.01 cm.

Longitudinal strains in the bar were calculated at the center and at the outer radius of the bar. The strains were calculated based on the relative displacements of two pairs of nodes. One pair of nodes was located at the outer radius of the bar, the other was at the radial center of the bar. Each pair of nodes was located so that one node was 0.8 mm below and the other was 0.8 mm above a longitudinal distance of 15.24 cm (6 inches) from the bottom of the bar. The 1.6-mm distance between the nodes represents a typical gauge length for strain gauges that are used experimentally to perform pressure measurements using Kolsky bars. The elastic strains ε were calculated as $\varepsilon = \ln [l(t) / l_0]$, where l_0 is the initial distance between the nodes and $l(t)$ is the distance between the nodes at time t. A diagram showing the layout of the bar and of the nodes used to measure the strain is shown in Fig. 4.

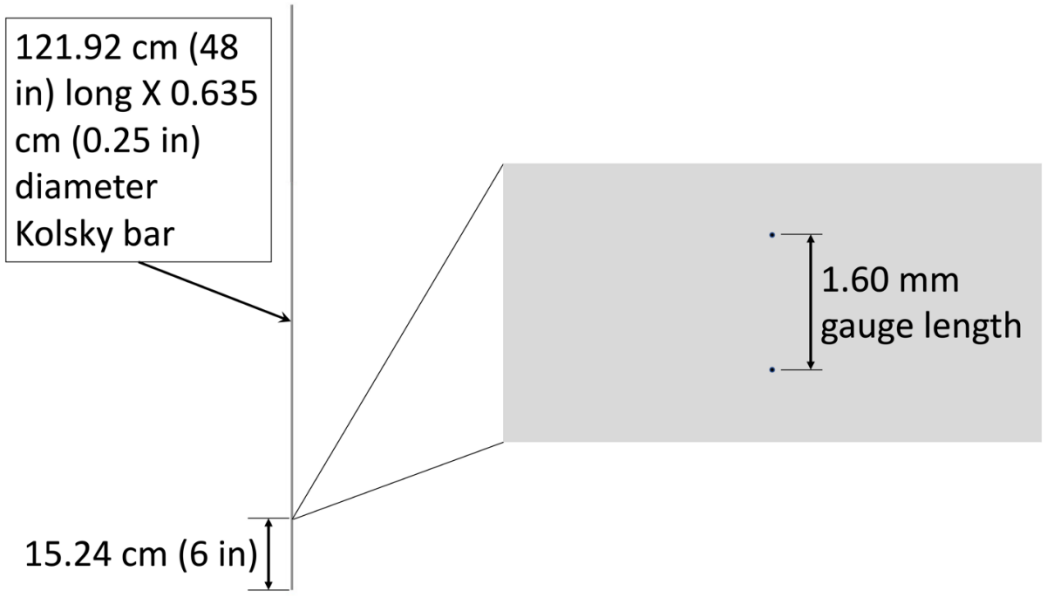


Fig. 4 Kolsky bar arrangement used for computations

Two types of synthetic input pressure pulses were applied to the bottom of the bars: a 20-μs-duration square wave and a 30-μs-duration pulse that was the product of a half sine and a decaying exponential given by $\sin(\pi\, t / 50) \times \exp(0.4\, t)$, where t is time in units of microseconds. The decaying exponential pulse was constructed to match the general shape of experimentally observed blast pulses. The amplitudes and durations of the pulses were varied based on the purpose of the analysis in which they were used. The two pulse types that were used are illustrated in Fig. 5.

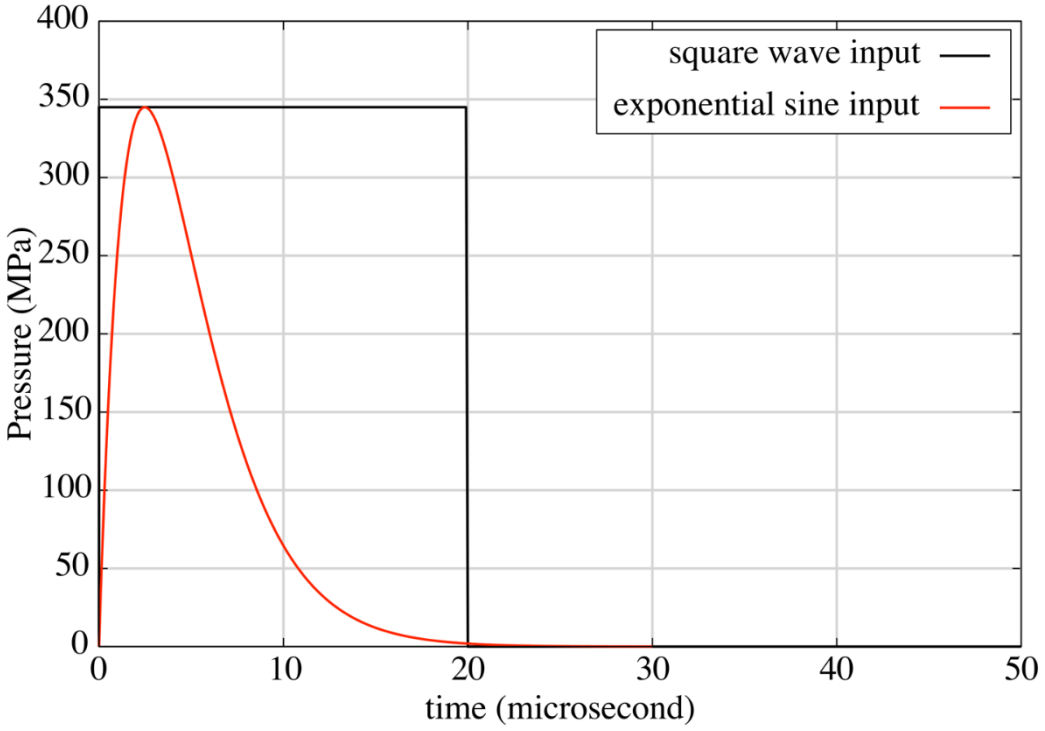


Fig. 5 Input pressure pulses that were applied uniformly to the bottom flat surfaces of the Kolsky bars. The amplitudes and durations of the pulses were varied to match the purpose of the analysis in which they were used.

2.2 Constitutive Models

Two types of material were used to model the bars. Care was taken to ensure that the peak stresses would be well below the reported yield strengths of the materials. As a result, the two metals that were used were modeled as linearly elastic–perfectly plastic solids.

The baseline bar material was a grade of maraging steel that is commonly used in Kolsky bar work: C350. The parameters used for density, Young's modulus, and Poisson ratio were 8,064 kg/m^3, 182 GPa, and 0.33,[17] respectively, and the value used for yield strength was 2.4 GPa.[18] Simulations were also performed that involved the use of beryllium. The density used for beryllium[19–21] was 1,850 kg/m^3, the Poisson ratio[20,21] was 0.03, and the Young's modulus and yield strength[22] were 3.105 GPa and 190 MPa, respectively

Three materials were used to simulate the behavior of the constraining sheaths used for the simulations in Section 3.4. The Teflon sheath was simulated using a Steinberg–Guinan model with a Grüneisen equation of state. The C350 maraging steel sheath used the same parameters as given above for the maraging steel used to model the Kolsky bar. The heavy tungsten alloy sheath was modeled using a

95% tungsten alloy with density[23] of 18,100 kg/m^3, Young's modulus 310.5 GPa, Poisson ratio 0.3095, and yield strength 110 GPa[24].

3. Results and Discussion

3.1 Radial Direction Displacement Constraints

Computations were performed to examine the way that maraging steel Kolsky bar radial displacement constraints would affect the measurement of applied input pressure signals. If constraints were applied to prevent radial movement of the bar's surface, it was possible to very closely reproduce the input exponential sine pressure signal (Fig. 6). The axial strain measurement in the unconstrained bar, at the outer radius of the bar, was converted to axial stress according to the relation $\sigma_a = E\varepsilon_a$ where σ_a is the stress in the axial direction, E is the Young's modulus, and ε_a is the axial strain. This is the relation that is generally used to convert strain to stress in unconstrained Kolsky bars. In the radially constrained bar, the strain signal was converted according to the relation $\sigma_a = M\varepsilon_a$, with the Young's modulus E replaced by the constrained modulus $M = E(1 - \nu)/[(1 + \nu)(1 - 2\nu)] = 2.70$ MPa (for C350 maraging steel) as is appropriate for the case of radially constrained 1-D transmission of waves, such as those associated with p-waves in earthquakes, through solid media. By way of comparison, it can be seen in Fig. 3 that the signal in the unconstrained bar showed differences in the shape and the peak of the signal when compared to the input signal. The Kolsky bar signals were shifted in time to allow a closer comparison between them and the input signal.

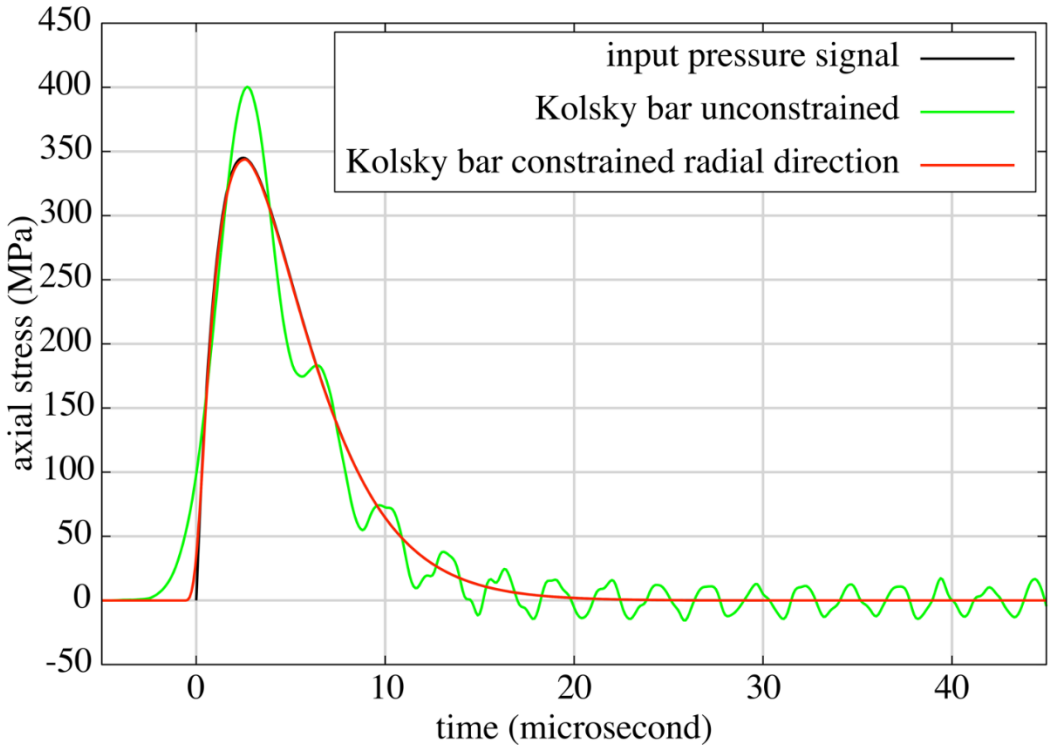


Fig. 6 Influence of constraint in the radial direction, at the outer radius of the C350 maraging steel Kolsky bar, on the accuracy of reproduction of the exponential sine input pressure signal with a peak amplitude of 345 MPa

The computations discussed previously showed that constraints that prevent radial displacements in Kolsky bars improve the accuracy of pressure signal measurement. As a result, various techniques for the mechanical suppression of radial displacement were pursued. Of those, two methods showed the most promise. The first method was relatively straightforward and involved using beryllium as the bar. The second approach that was discovered, the windowed constraint method, used a mechanical means for constraint, in the radial direction, of a finite length of the bottom of the bar with an unconstrained window in the constrained portion of the boundary of the bar that could be used to measure the longitudinal strain signal.

3.2 Beryllium Kolsky Bars

The Poisson ratio is a measure of the degree to which solids deform in a direction normal to the direction of mechanical loading. The Poisson ratio of beryllium is an order of magnitude lower than that of most other solid materials that might be used in a Kolsky bar. By virtue of the relatively small value for Poisson ratio of beryllium, the amount of radial displacement and dispersion induced in a beryllium Kolsky bar by a blast pressure signal applied to the bottom of a bar would be

expected to be considerably lower than what would be observed using a bar composed of most other materials.

Computations were performed to compare the exponential sine input pressure signal, the response of a beryllium Kolsky bar, and the response of a bar made with maraging steel. Figure 7 shows the results of this comparison. In Fig. 7, the Kolsky bar strain gauge signals were shifted in time to allow a better comparison between them and the input signal. As was observed in the previous computations, the strain gauge signal produced by means of the maraging steel bar deviated from the input signal both in its peak value and in its shape. However, it was observed that the low Poisson ratio of the beryllium Kolsky bar enabled the measurement of a pressure signal that was nearly identical to the input pressure signal.

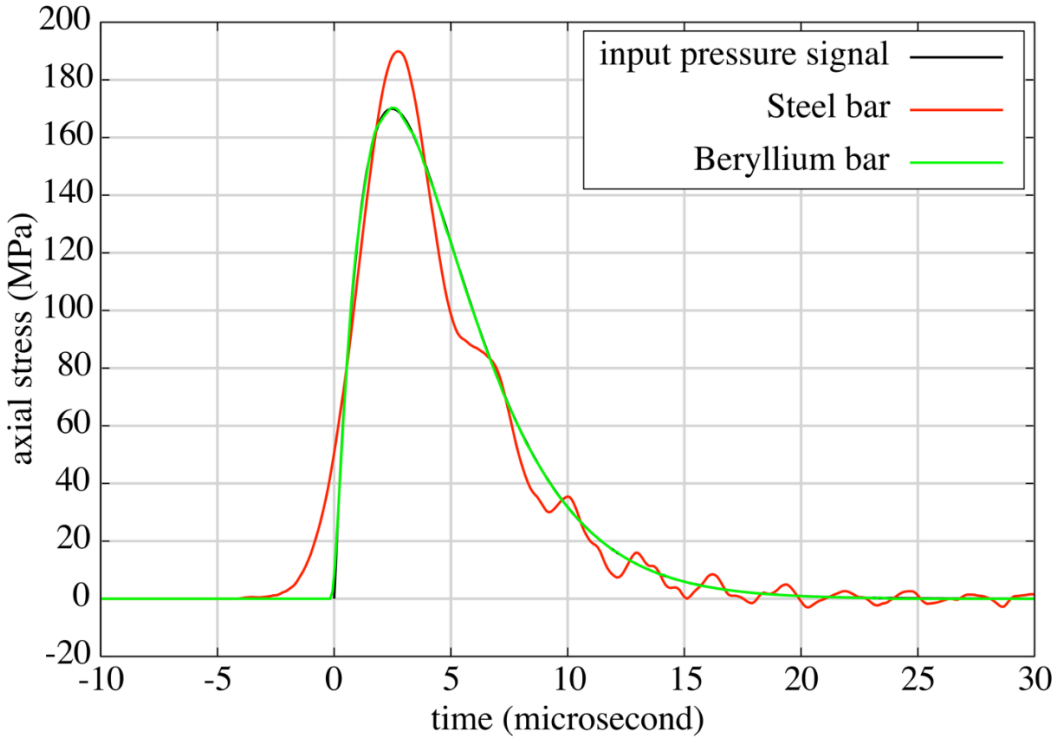


Fig. 7 Beryllium Kolsky bars improve signal measurement. The Kolsky bar signals were shifted in time to allow a closer comparison between them and the 170-MPa peak pressure input signal.

These computations clearly demonstrate that the use of beryllium as the material of construction for Kolsky bars offers a direct approach to treating blast pressure signal distortion due to dispersion effects. However, it should be noted there are two important factors to consider if beryllium is to be used in Kolsky bars for blast pressure measurement. First, the relatively low yield strength—190 MPa as compared with 2.40 GPa for C350 maraging steel—will place a lower limit on the peak blast pressures that can be measured by means of beryllium Kolsky bars. This

was why 170 MPa was chosen as the peak pressure for the input signal used for the simulations that were used to create Fig. 7 rather than 345 MPa, the peak pressure used for the other computations in this report. Also, beryllium, particularly when powdered or fractured, is known to be a hazardous material if not handled properly, so its use for pressure measurement using Kolsky bars would require special precautions to ensure safety.

3.3 Windowed Radial Constraint

A second method for mechanical reduction of signal degradation due to dispersion was discovered. The configuration of a Kolsky bar that applies this technique is shown in Fig. 8. The configuration of the bar is identical to that of the bars used earlier with respect to its length, its diameter, and the positions of the nodes used to calculate strain at the outer diameter of the bar. However, for this particular configuration of the bar, the bottom 30.38 cm of the bar is constrained, at the outer diameter, in such a way that the bar is able to deform longitudinally but is constrained against displacement in the radial direction.

In the midst of this constrained region, there is a window for measurement of the strain signal. This window is not constrained in the radial or longitudinal directions and is 2.20 mm high by 0.79 mm wide. The longitudinal center of the measurement window is located 15.24 cm (6 inches) above the bottom of the bar.

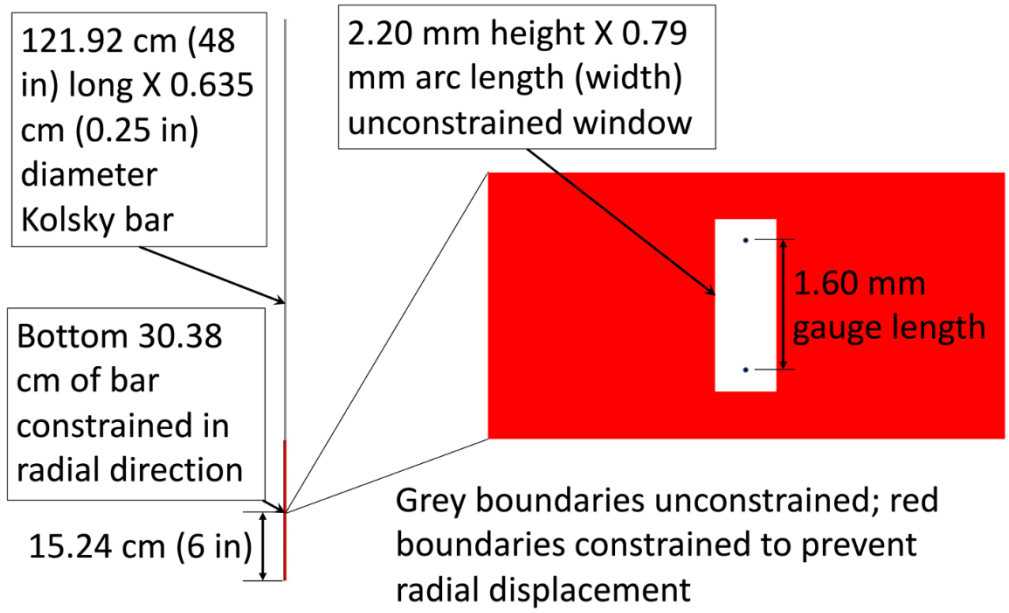


Fig. 8 Geometric configuration of a Kolsky bar that is set up to mechanically suppress blast pressure measurement degradation due to dispersion effects

For bars that were made from C350 maraging steel, the radial constraint along the first 30.38 cm of the bar suppressed most, but not all, of the displacements in the radial direction. A lack of radial constraint along the measurement window created a minor amount of signal distortion. Computations were performed for which the exponential sine input signal amplitude varied between 150 and 900 MPa. It was observed that if the constrained modulus M—270 MPa for C350 steel—was used to convert the strain signal to a stress signal, the calculated pressure values were somewhat low. However, it was determined by comparing the peak strains and the peak input pressure values that if a slightly higher value for the proportionality constant between stress and strain—M' = 290 MPa—was used to convert the strain signals to stress signals, then the peak pressures, as well as the shapes of the converted strain pulses measured in the unconstrained window, very closely matched the peak values and shapes of the input pressure pulses for the entire range of peak pressures that were studied. Figure 9 compares the measured peak pressures against the input peak pressures for the range of input pressures that were examined.

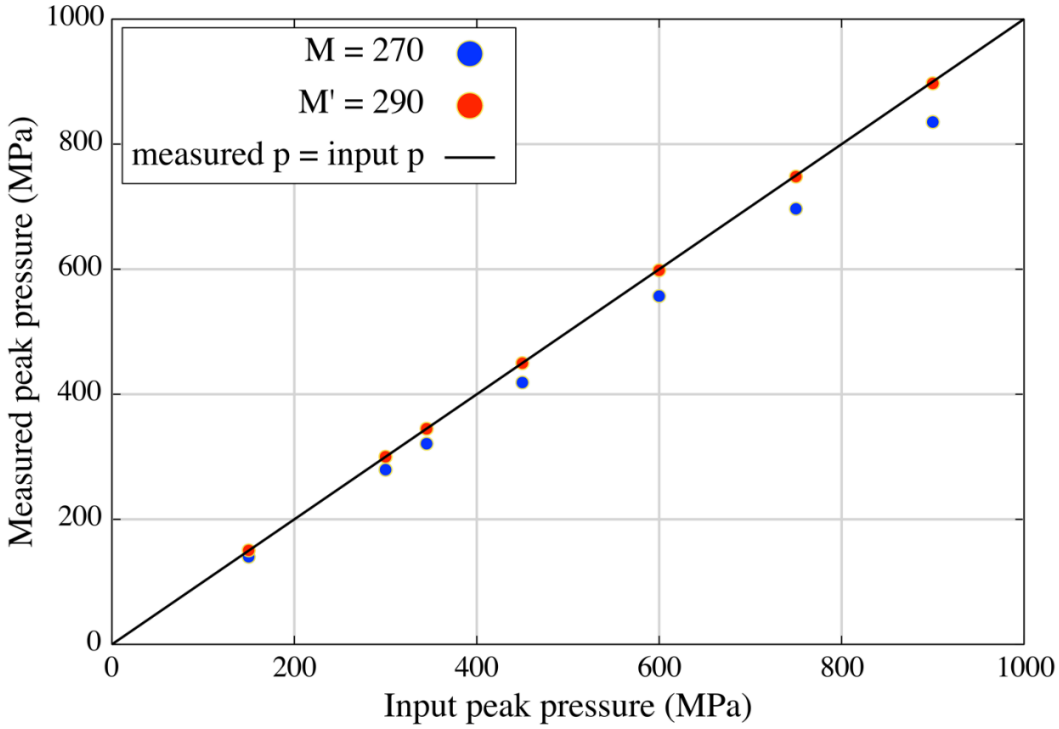


Fig. 9 Comparison of measured peak pressure calculated by converting the peak longitudinal strain to stress using the constrained modulus M for C350 steel (270 MPa) and the measured peak pressure using an adjusted constrained modulus M' (290 MPa)

In Fig. 10, an input exponential sine pressure input signal with a peak of 345 GPa is compared with C350 maraging steel Kolsky bar pressure signals using the windowed constraint method as well as with maraging steel Kolsky bar unconstrained output signals. It can be seen that the windowed constraint method

produced a pressure output that varied little, in shape or peak pressure value, from the input signal, whereas the signal from the unconstrained Kolsky bar deviated from the input signal as a result of dispersion and spurious radially dependent signal variations.

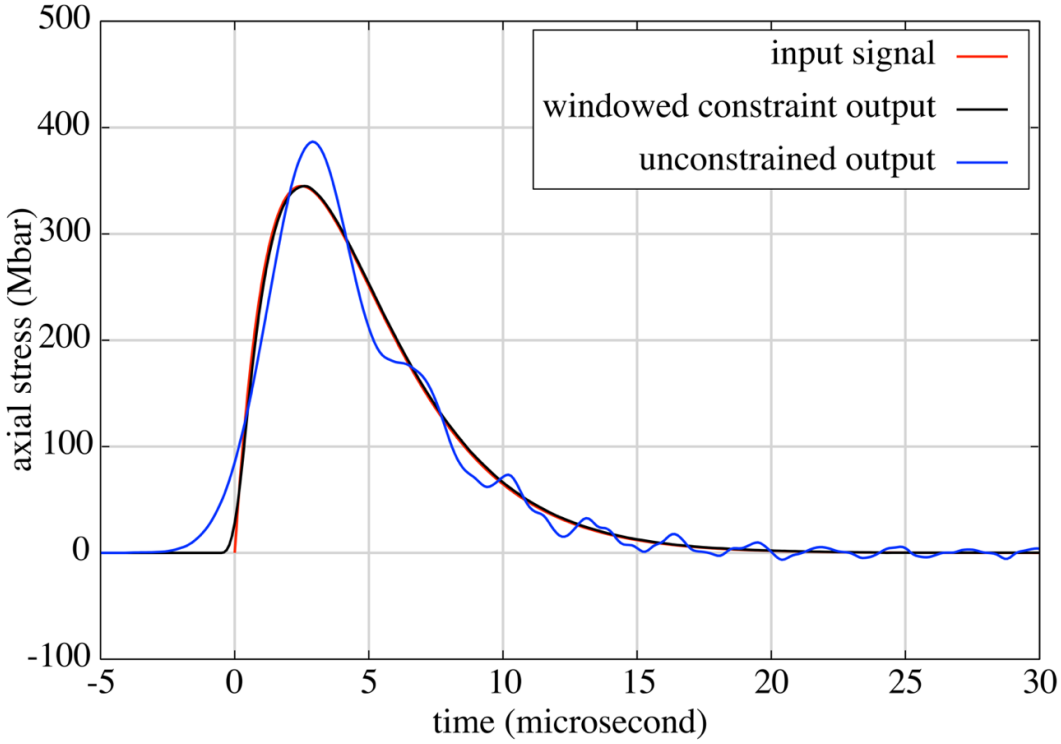


Fig. 10 Comparison of input pressure signal, windowed constraint C350 maraging steel Kolsky bar, and traditional unconstrained Kolsky bar responses to 345-GPa peak exponential sine signal pressure input

Figure 11 shows a similar result for Kolsky bar responses to a 345-GPa peak square wave input pressure signal. The signal generated via the bar that used the windowed constraint method produced a pressure output that closely matched the input signal; whereas, the unconstrained Kolsky bar signal was different from the input signal. The computational results shown in Figs. 9, 10, and 11 demonstrate that the windowed radial constraint method could offer an effective means for improvement of the accuracy of blast pressure measurement using Kolsky bars.

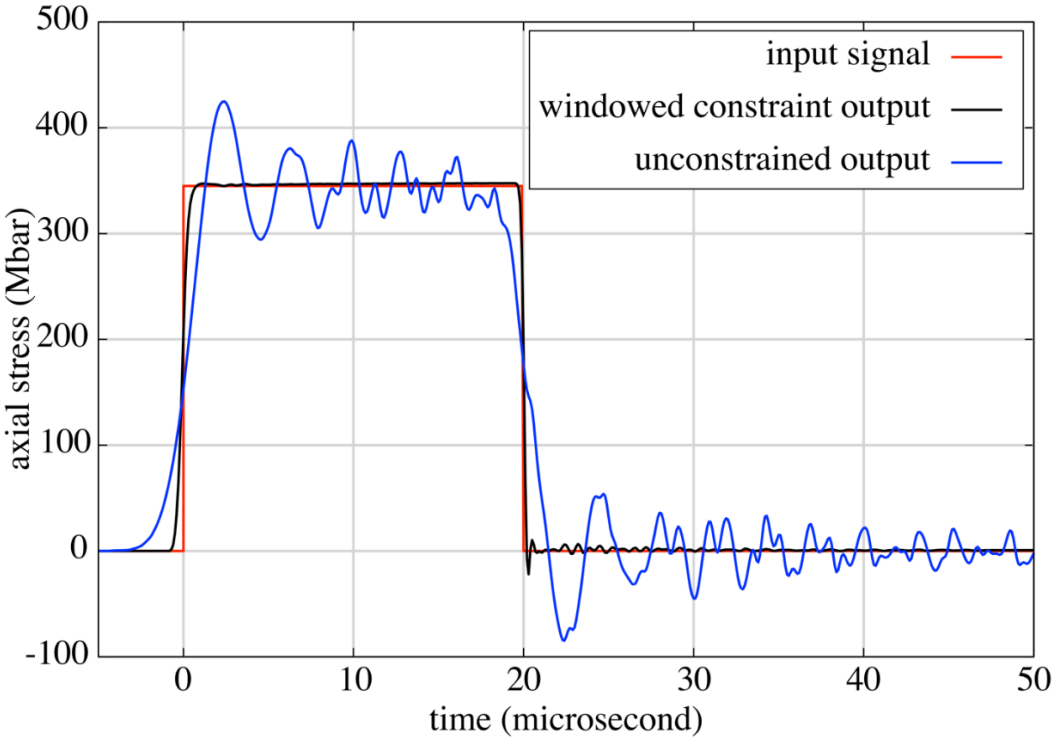


Fig. 11 Windowed constraint C350 maraging steel Kolsky bar and traditional unconstrained Kolsky bar responses to 345-GPa peak square wave pressure input

3.4 Kolsky Bar Sheath Radial Constraints

Based on the results discussed in Section 3.3, computational models were used to perform initial evaluations of the effectiveness of 1.25-cm outer diameter, 3.075-mm-thick annular sheaths for reduction of pressure signal errors due to dispersion. As such, 30.38-cm-high annular sheaths were placed at the bottoms of the bars in the position shown for the radial constraints in Fig. 8. The sheaths were modeled as being in direct contact with the outer radii of the C350 maraging steel Kolsky bars and were constructed of Teflon, C350 maraging steel, or heavy tungsten alloy with 95% tungsten content. They were modeled with a frictionless contact so that the sheaths provided some radial constraint of the Kolsky bars but did not restrict vertical movement between the bars and the sheaths. For the purposes of this initial investigation of sheath performance, it was assumed that it should be possible in the future to isolate the bottoms of the sheaths from the blast loading so the input pressure signal was applied to the bottom of the Kolsky bars but not to the bottoms of the sheaths in order to simplify the analysis. The measured pressures from these simulations, taken at a distance of 15.24 cm from the bottoms of the bars, are shown in Fig. 12.

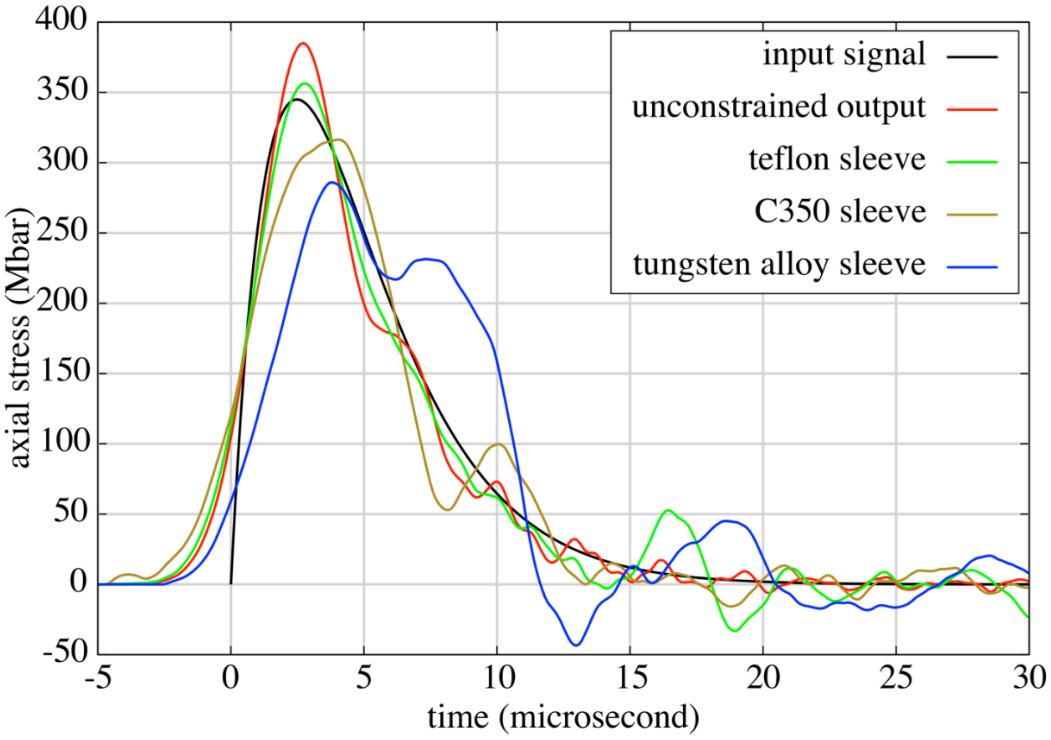


Fig. 12 Comparison of computational pressure–time histories measured using unconstrained bars with those measured with bars sheathed at their bottoms with 3.075-mm-thick annuli of Teflon, C350 maraging steel, or heavy tungsten alloy

In Fig. 12, it can be seen that the bars with C350 maraging steel and tungsten alloy constraining sheaths yielded peak pressures of 316 and 286 MPa, respectively, and attenuated the peak pressures by about 17% and 8%, respectively, as compared to the 345-MPa input peak pressure. The bars with the steel and tungsten alloy sheaths also added spurious oscillations to the measured pressure signals. The Teflon sheath yielded a measured peak pressure of 356 MPa, which was about 3% higher than the peak input pressure. The peak pressure measured with the unconstrained bar was 385 MPa and was about 12% higher than the input peak pressure. It can also be seen that although there were some oscillations due to reflections in the Teflon sheath that began to show up at about 13 μs on the Fig. 12 timescale, the Teflon sheath removed many of the signal oscillations due to dispersion that were observed with the unconstrained bars.

It was suspected that an increase of the Teflon sheath thickness might delay the onset of the oscillations that began to occur at about 14 μs on the Fig. 12 timescale. To explore this further, simulations were run using a Teflon sheath with an outer diameter of 1.875 cm and it was observed that an increased sheath diameter improved the measured pressure signal by delaying the spurious oscillations almost to the end of the measured pressure signal (Fig. 13). In Fig. 13, it can be seen that

signals generated with Teflon sheaths of both outer diameters were almost identical until about 11 μs, at which point they diverged with the thicker sheath yielding, until about 24 μs, a signal with obvious reduction of oscillations due to dispersion when compared with the output from the unconstrained bar.

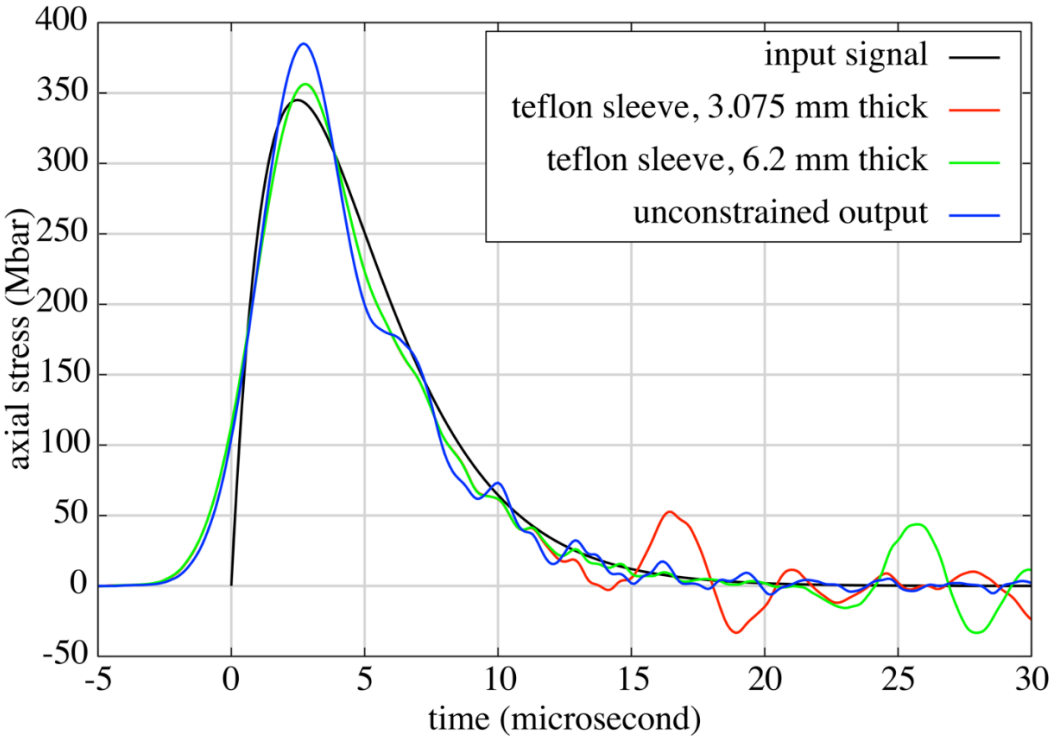


Fig. 13 The effect of increasing the thickness of the constraining Teflon sleeve from 3.075 to 6 mm

4. Summary and Conclusions

Analytical and numerical methods have been devised that could be used to improve blast pressure measurement accuracy. This report used computational methods to examine and illustrate two novel approaches to the improvement of Kolsky bar pressure measurements that show substantial potential for reducing measurement error.

Both approaches used direct mechanical means to remove signal distortions due to dispersion in Kolsky bars. The first method involved replacing standard Kolsky bar materials of construction such as maraging steel or titanium alloy with beryllium. Beryllium, by virtue of its extremely low 0.03 Poisson ratio, provided a direct means for suppression of displacement in the radial direction of the bar and, as a result, was able to virtually eliminate signal distortion caused by dispersion. Although beryllium has a yield strength that is lower than that of commonly used

bar materials and can be toxic if not handled appropriately, it has found use in many applications. This approach is ready for a transition to implementation in experimental blast pressure measurement work.

A second approach explored used radial boundary constraints for the mechanical suppression of radial displacements in Kolsky bars. This method involved mechanical constraint in the radial direction at the outer radius of a section of a cylindrical Kolsky bar. This method was shown to be effective at suppressing dispersion and radial signal variation, thereby enabling improved measurement accuracy.

An initial computational investigation was performed to look at the use of annular sheaths made of various materials to constrain the radial displacement of the bars. The difference between peak pressure measured by an untreated Kolsky bar and peak input pressure was about 12%. This difference was reduced to about 3% with use of an annular Teflon sleeve applied to the outer boundary of a Kolsky bar. It was also found that, as compared to the untreated Kolsky bar, the Teflon sheath visibly reduced spurious oscillations caused by dispersion.

5. References

1. Hopkinson B. A method of measuring the pressure produced in the detonation of high explosives or by the impact of bullets. Philos Trans Roy Soc Lond Ser. A 1914;213(1914):437–56.

2. Taylor LC, Fourney WL, Leiste HU. Pressures on targets from buried explosions. Int J Blast Fragm. 2010;4(3):165–92.

3. Clarke S, Fay S, Warren J, Tyas A, Rigby S, Elgy I. A large scale experimental approach to the measurement of spatially and temporally localised loading from the detonation of shallow-buried explosives. Measur Sci Technol. 2015;26:015001.

4. Leiste UH. Experimental studies to investigate pressure loading on target plates [dissertation]. University of Maryland; 2012.

5. Pochhammer L. Über die fortpflanzungsgeschwindigkeiten kleiner schwingungen in einem unbegrenzten isotropen kreiszylinder. Journal für die reine und angewandte Mathematik 1876;81:324–36.

6. Chree C. The equations of an isotropic elastic solid in polar and cylindrical coordinates. Trans Camb Philos Soc. 1889;14:250–369.

7. Bancroft D. 1941 Phys. Rev. 59 588–93.

8. Davies RM. A critical study of the Hopkinson Pressure Bar. Philos Trans Roy Soc Lond Ser. A 1948;240(821):375–457.

9. Gorham DA. A numerical method for the correction of dispersion in pressure bar signals. J Phys. E 1983;16:477–9.

10. Follansbee PS, Frantz C. Wave propagation in the Split Hopkinson Pressure Bar. Journal of Engineering Materials and Technology. 1983;105:61–6.

11. Tyas A, Watson AJ. An investigation of frequency domain dispersion correction of pressure bar signals. Int J Impact Eng. 2001;25(1):87–101.

12. Barr AD, Rigby, SE, Clayton, M. Correction of higher mode Pochhammer–Chree dispersion in experimental blast loading measurements, A.D. Barr, S.E. Rigby, M. Clayton, Correction of higher mode Pochhammer–Chree dispersion in experimental blast loading measurements. Int J Impact Eng. 2020;139: 103526.

13. Fox D. The effect of Kolsky bar diameter, charge size, and distance from an explosive charge on the measurement of local pressure from a buried blast. Army Research Laboratory (US); 2019 Aug. Report No.: ARL-TR-8775.

14. Bateman VI, Davie NT, Brown FA. Characteristics of a piezoresistive accelerometer in shock environments up to 150,000 G. Annual Technical Meeting and Exposition of the Institute of Environmental Sciences; 1–5 May 1995; Anaheim, CA.

15. Tyas A, Watson AJ. A study of the effect of spatial variation of load in the pressure bar. Meas Sci Technol. 2000;11:1539–1551.

16. Nichols AL, Dawson DA. ALE3D user's manual. Version 4.30.29. Lawrence Livermore National Laboratory; 2018. Report No. LLNL-SM-750117.

17. Bolduc M, Arsenault R. Improving accuracy in the Split Hopkinson pressure bar. DRDC Valcartier (CANADA); 2008. Report No.: TR 2005–380.

18. Rohrbach K, Scmidt M. Maraging steels. In: Properties and selection: irons, steels, and high-performance alloys. ASM International; 1990.

19. Steinberg DJ. Equation of state and strength properties of selected materials. Lawrence Livermore National Laboratory; 1996. Report No. UCRL-MA-106439 Change 1.

20. Christman DR, Feistmann FJ. Dynamic properties of S-200-E beryllium. General Motors Technical Center; 1971. Report No. MSL-71-23.

21. Igonin VV. Beryllium dynamic strength measurements: Report on Task 3 Agreement #B590737. Lawrence Livermore National Laboratory; 2014. Report No. LLNL-TR-653180.

22. Goldberg A. Atomic, crystal, elastic, thermal, nuclear, and other properties of beryllium. Lawrence Livermore National Laboratory; 2004. Report No. UCRL-TR-224850.

23. Senf H., et al. Investigation of the ballistic resistance of ceramic/steel targets versus short tungsten alloy rods. Ernst Mach Institute; 1995. Report No. EMI 11/95.

24. Bruchey WJ, Montiel DM. Mechanical property evaluation of a series of commercial tungsten alloys. Ballistic Research Laboratory (US); 1987 Jun. Report No.: BRL-MR-3606.

1 (PDF)	DEFENSE TECHNICAL INFORMATION CTR DTIC OCA
1 (PDF)	DEVCOM ARL FCDD RLD DCI TECH LIB
23 (PDF)	DEVCOM ARL FCDD RLW TB S SATAPATHY FCDD RLW TC J CAZAMIAS D CASEM C MEREDITH L SHANNAHAN FCDD RLW TG N GNIAZDOWSKI D ABELL C ADAMS J ANDERSON C CUMMINS J CROOKSHANKS P DUVALL E FIORAVANTE D FOX D HOFSTETTER S HUG S KOUNDINYAN S KUKUCK T PAYNE C PECORA J PRITCHETT J STEWART S TROMBETTA